CARBON letters

Original Articles
Carbon Letters Vol. 15, No. 1, 50-56 (2014)

Water and oxygen permeation through transparent ethylene vinyl alcohol/(graphene oxide) membranes

Hye Min Kim[1,2] and Heon Sang Lee[2,♠]

[1]Sangbo Co., LTD., Suwon 443-270, Korea
[2]Department of Chemical Engineering, Dong-A University, Busan 604-714, Korea

Article Info
Received 4 November 2013
Accepted 9 December 2013

***Corresponding Author**
E-mail: heonlee@dau.ac.kr

Open Access
DOI: http://dx.doi.org/10.5714/CL.2014.15.1.050

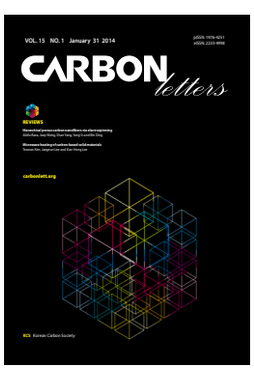

http://carbonlett.org

pISSN: 1976-4251
eISSN: 2233-4998

Abstract

We prepared ethylene vinyl alcohol (EVOH)/graphene oxide (GO) membranes by solution casting method. X-ray diffraction analysis showed that GOs were fully exfoliated in the EVOH/GO membrane. The glass transition temperatures of EVOH were increased by adding GOs into EVOH. The melting temperatures of EVOH/GO composites were decreased by adding GOs into EVOH, indicating that GOs may inhibit the crystallization of EVOH during non-isothermal crystallization. However, the equilibrium melting temperatures of EVOH were not changed by adding GOs into EVOH. The oxygen permeability of the EVOH/GO (0.3 wt%) film was reduced to 63% of that of pure EVOH film, with 84% light transmittance at 550 nm. The EVOH/GO membranes exhibited 100 times better (water vapor)/(oxygen) selectivity performance than pure EVOH membrane.

Key words: graphene oxide, ethylene vinyl alcohol, permeability, selectivity, water vapor

1. Introduction

Ethylene vinyl alcohol (EVOH) is one of the best known oxygen barrier materials in use today, with excellent gas barrier properties, processability, and sensitivity to moisture [1-3]. The permeation of oxygen and water vapor can lead to damage in electronic devices and the decomposition of foods. Barrier films can enhance the lifetime of electronic devices, and are required for food packaging or volatile solvents packaging and moisture sensitive products.

Graphene has been known to serve as an atomic impermeable membrane [4-7]. Graphene oxide (GO) is the intermediate for graphene, and can be obtained by chemical oxidation of natural graphite [8-10]. Kim and coworkers [10] were the first to demonstrate that the oxidative form of graphene (GO) is itself an excellent gas barrier to oxygen. Subsequently, Nair and coworkers [4] have reported that helium permeation is inhibited by GO but water permeation is not impeded by GO.

Yang and coworkers [11] have shown that a polyethyleneimine (PEI)/GO multilayer membrane exhibits good oxygen/hydrogen selectivity. For a transparent oxygen barrier, poly(vinyl alcohol) (PVA)/GO membranes are the best among the reported membranes consisting of GO and polymers [10]. The oxygen transmittance rate (OTR) in PVA/GO (0.3 wt%) composite coated film has been reported to be 86 times lower than that of pure polyethylene terephthalate (PET) film, at 60% relative humidity (RH), with 73% light transmittance [10]. Thirty layered PEI/GO membrane has been reported to have 18 and 45 times lower OTR than pure PET film at 100% RH and 0% RH, respectively [11]. Gas barrier properties of various polymer/GO membranes have also been reported for polymers such as PVA [10], polyurethane [12], polycarbonate [13], and poly(ethylene terephthalate) [14].

Gas permeability (P) is the product of diffusivity (D) and solubility (S) which can be obtained from the solution of Fick's second law of diffusion as described elsewhere [10,15,16]. In our previous work, we showed that both the D and S of oxygen are decreased by dispers-

ing GOs into PVA [10]. The decrease of D is mainly due to the increase of effective diffusion path; tortuous paths are formed by the dispersed GO plates [10,16]. We can expect that the D of water vapor may be decreased by the dispersion of GOs into a polymer, but the S of water vapor may be increased due to the hydrophilic nature of GO. Therefore, composites of polymer and GO could be a potential material for a water/gas selective membrane. Selectively permeable membranes for gas/water vapor are known to be used in various applications such as the drying of compressed air [17], drying of natural gas [18,19], breathable apparel [20], packaging materials [21], and humidity control in a closed space [22,23].

In this work, we prepared transparent and flexible EVOH and GO membranes by solution casting method in order to check their barrier properties to oxygen and water. We demonstrated that the oxygen permeation of EVOH is reduced remarkably by adding GOs into EVOH, while water permeation of EVOH is increased by the addition of GOs into EVOH. EVOH/GO membranes exhibited 100 times improved (water vapor)/(oxygen) selectivity compared to pure EVOH membrane. These results point to new possible applications of EVOH/GO films as an oxygen/water selective membrane.

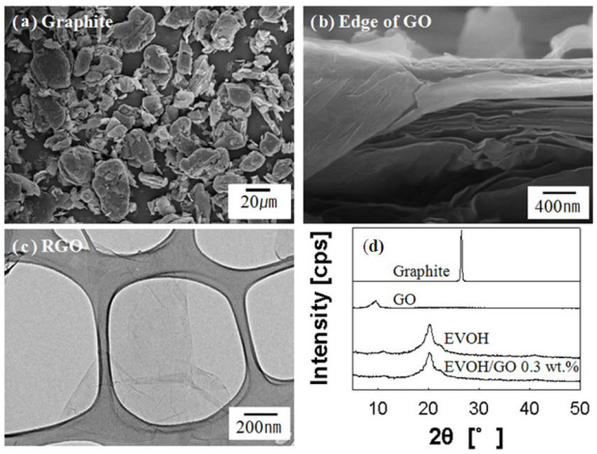

Fig. 1. Morphology of graphite, graphene oxide (GO) and reduced GO. (a) Scanning electron microscope (SEM) image of graphite. (b) SEM image of edge of dried GO. (c) Transmission electron microscope image of reduced GO (RGO). (d) The X-ray diffraction patterns of graphite, GO, and ethylene vinyl alcohol (EVOH)/GO composite.

2. Experimental

2.1. Preparation of GO

Flake graphite powder (19 μm nominal particle size) was supplied from Asbury Carbon. GO was synthesized from purified conventional flake graphite by modified Hummers method [8,9] as reported in our earlier work [10].

2.2. Preparation of EVOH/GO film

EVOH (32 mol % ethylene) was supplied from Kuraray. EVOH/GO nanocomposites were prepared by solution mixing method, of EVOH in a colloidal solution of GO. EVOH (3 g) was dissolved in distilled water and isopropyl alcohol (IPA) (water/IPA weight ratio = 1) at 353.15 K and the solution cooled to 313.15 K. A colloidal solution of GO was added to the EVOH solution and mixed for 24 h at 313.15 K. EVOH/GO hybrid solution was cast onto PET film at 363.15 K and then dried for 1 h. The films were dried again in a vacuum oven at 373.15 K for 4 h. A series of EVOH/GO nanocomposite films with different GO loadings were similarly prepared. EVOH/reduced GO (RGO) solutions were synthesized by chemical reduction using hydrazine monohydrate. Hydrazine solution was added to the EVOH/GO solution and mixed for 24 h.

2.3. Characterization methods

The interlayer spacing of graphite and GO and the dispersion of GO in EVOH composite were characterized with X-ray diffraction (XRD). XRD was conducted with a Rigaku (Japan)-Ultima IV (40 kV, 40 mA) and Cu irradiation at the scanning rate of 0.02 /s in the 2θ range of 5-70. The light transmittance of the nanocomposite films was measured with UV-vis at 550 nm. The morphologies of the nanocomposites were characterized with field-emission scanning electron microscopy (FE-SEM, JEOL JSM-6700F) and high-resolution transmission electron microscopy (HRTEM, JEOL JEM-2010). For preparation of TEM samples, RGO solution was dropped onto a 400-mesh Cu grid covered with lacey carbon film and dried at room temperature. Nominal melting temperatures of the samples were measured by differential scanning calorimeter (DSC-Q10) with a heating rate of 20 K/min. In order to measure the melting temperatures of isothermally crystallized samples, the samples were heated up to 483 K and held there for 5 min, and then cooled quickly (-80 K/min) to the designated crystallization temperature. When the isothermal crystallization procedure was finished, the samples were heated again with a heating rate of 20 K/min. The OTR of films (dimension 10 × 10 cm) was measured with Illinois Instrument Model 8001. The water vapor transmission rate of films (dimension 10 × 10 cm) was measured with Permatran-W 3/33 MA (US, Mocon) according to the standard test method ASTM F 1249.

3. Results and Discussion

3.1. Morphological characterization

Fig. 1a shows the morphology of graphite, with a nominal particle size of 19 μm. We prepared the GOs from graphite by the modified Hummers method [8-10]. The FE-SEM image of the edge of dried GOs is shown in Fig. 1b. The layered structure of the dried GOs can be seen. We prepared a RGO solution by using hydrazine monohydrate for the chemical reduction. Fig. 1c shows the electron transparency of RGO sheets on lacey carbon grid, showing the typical image of graphene. Fig. 1d shows the XRD patterns of graphite, dried GO, EVOH and EVOH/GO composite (GO 0.3 wt%). A sharp reflection is seen at 2θ = 26.4° for graphite powder, which corresponds to the interlayer spacing (d) of 0.34 nm. The broad peak of dried GO particle is present

Table 1. Thermal properties of EVOH/GO and EVOH/RGO composites

GO/RGO (wt%)	T_g (K)[a]	T_c (K)[a]	T_m (K)[a]	T_m^0 (K)[b]
0	334.6	432.3	456.8	459.4
GO 0.01	336.5	429.4	457.4	-
GO 0.3	336.2	423.5	448.4	456.9
RGO 0.01	333.0	432.4	455.6	-
RGO 0.3	336.2	431.2	456.8	456.9

EVOH: ethylene vinyl alcohol, GO: graphene oxide, RGO: reduced GO.
[a]Non-isothermal glass transition temperatures (T_g) and melting temperatures (T_m) were measured during second heating. Non-isothermal crystallization temperatures (T_c) were measured during cooling at a rate of 20 K/min.
[b]Equilibrium melting temperatures.

at 2θ = 9.5°. The interlayer spacing of GO is 0.93 nm, indicating the intercalation by oxygen groups and moisture in GO sheets. The characteristic GO peak at 9.5° is absent for the EVOH/GO composite, but characteristic peaks of only EVOH in Fig. 1d indicate the exfoliation of GO in EVOH [10,24]. There is a sharp peak at 20.1° and broad peaks at 11.1°, 22.2°, and 35-45°, indicating the crystallization of EVOH. The XRD pattern of EVOH has a definite shoulder peak at 22.2°, which is the characteristic of atactic EVOH [10,25].

3.2. Thermal properties of EVOH/GO and EVOH/RGO composites

We investigated the thermal properties of EVOH/GO and RGO composites by differential scanning calorimeter. The glass transition temperature of pure EVOH is about 334.6 K, as shown in Table 1. The glass transition temperature of EVOH/GO and RGO composites was increased about 1.6 K by adding GO or RGO 0.3 wt% into EVOH. The increase of glass transition temperature may be due to the hydrogen bonding interaction between GO or RGO and EVOH [10].

The nominal melting temperature of EVOH/GO composites was decreased by adding GOs into EVOH, as shown in Fig. 2a. These results are in contrast to the results of PVA/GO [10]. The decrease of melting temperature of EVOH/GO composites may indicate that GO inhibits the crystallization of EVOH. However, the nominal melting temperature of EVOH/RGO is almost constant over the composition range from zero to 0.3 wt%. This result may be due to the reduced hydrogen bonding interaction between the EVOH and RGO compared to those in EVOH/GO composites. X-ray photoelectron spectroscopy analysis showed that the carbon to oxygen ratio of GO and RGO is 1.81 and 6.39, respectively. So, we can surmise that the hydrogen bonding interaction in EVOH/RGO composite is weaker than that in the EVOH/GO composite, which results in the different melting behavior in Fig. 2a.

In order to obtain the equilibrium melting temperatures of EVOH/GO and EVOH/RGO composites, we performed Hoffman-Weeks plots [26] as seen in Fig. 2b. The equilibrium melting temperatures of EVOH were not changed by the addition of GOs or RGOs. These results are consistent with those of PVA/GO composites. However, the slopes in the Hoffman-Weeks plots are increased by the addition of GO and RGO into EVOH, as seen in Fig. 2b. The increase of slopes may be due to the fact that the surface energy of crystalline EVOH may be decreased by the hydrogen bonding interaction between the crystal surface and GO [27]. Another possible reason for the increase of slopes is that the critical nucleus size of EVOH may be increased by the GO or RGO [27].

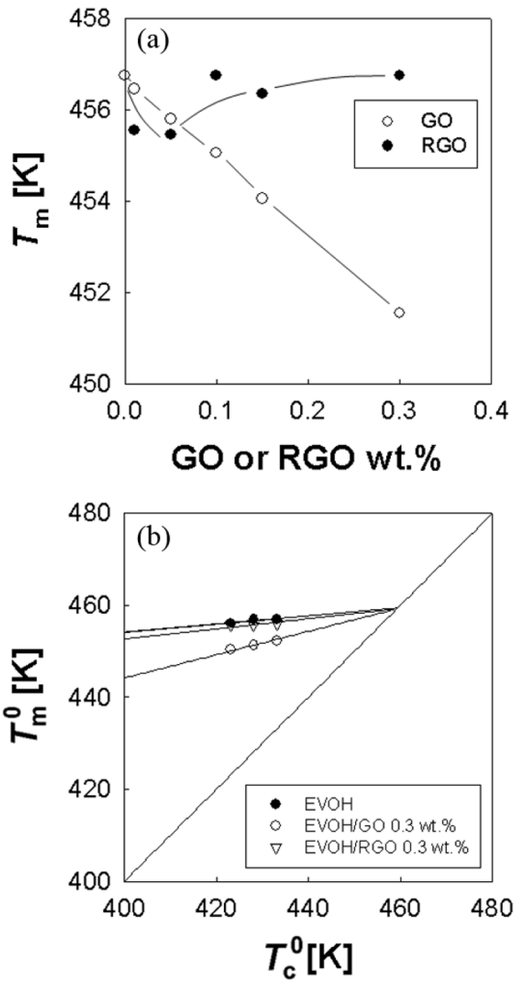

Fig. 2. Melting temperatures of ethylene vinyl alcohol (EVOH)/graphene oxide (GO) and reduced GO (RGO) composites. (a) Nominal melting temperatures of EVOH/GO or EVOH/RGO composites. (b) Equilibrium melting temperatures of EVOH/GO and EVOH/RGO composites.

3.3. Permeation of oxygen and water vapor

To study the oxygen and water vapor barrier properties, 12 μm EVOH/GO and EVOH/RGO composite films were coated on a 23 μm PET substrate using the bar-coating method. As can be seen from an optical picture in Fig. 3a, the film (GO 0.15 wt%) is very transparent. The light transmittance of the film was measured by UV-vis at 550 nm. In Fig. 3b, light transmittance is 95.8% for the EVOH/GO composite film containing 0.1 wt% GO and 84.8% for the film containing 0.3 wt%. With increasing

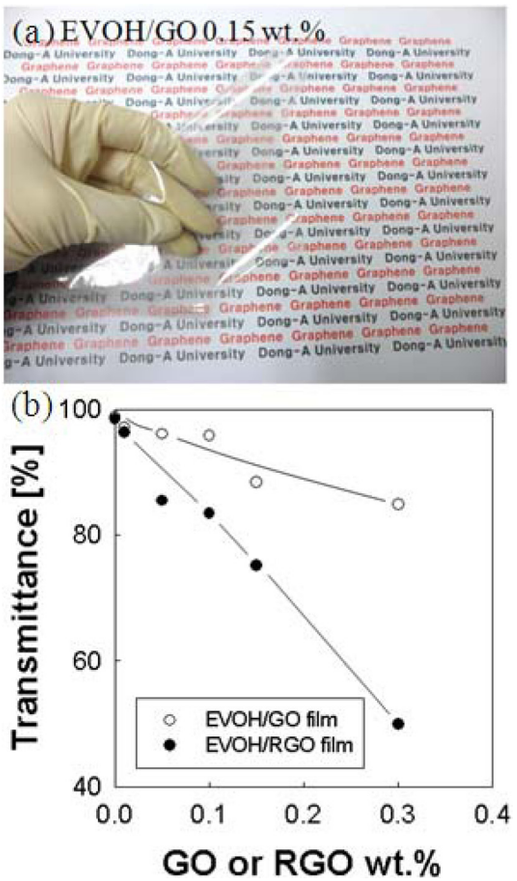

Fig. 3. Transparent ethylene vinyl alcohol (EVOH)/graphene oxide (GO) coated on polyethylene terephthalate (PET) film. (a) Picture of EVOH/GO coated PET film. (b) Light transmittance of EVOH/GO and EVOH/reduced GO (RGO) coated PET film at 550 nm.

GO and RGO contents, the light transmittance gets lower. After chemical reduction, the color of the film is changed from bright brown to dark brown. The oxygen permeability of the film was measured at 298 K and 60% RH. The oxygen permeability can be analyzed using Fick's second law of diffusion [10,15]:

$$D\nabla^2 c = \frac{\partial c}{\partial t} \tag{1}$$

where c is the oxygen concentration in the film. When the c is close to zero at the bottom surface, the solution of Eq. (1) can be expressed as follows [10,28,29].

$$J = J_s\left(\frac{4d^2}{\pi Dt}\right)^{0.5}\sum_{n=0}^{\infty}\exp\left[-\frac{d^2}{4Dt}(2n+1)^2\right] \tag{2}$$

where J and J_s are the oxygen molar flux at time t and at steady state, and d is the sample thickness. The solubility (S) is defined as the ratio of saturated oxygen concentration to the partial pressure (P) on the upper side of film [10].

$$S = c^*/p \tag{3}$$

$$P = SD \tag{4}$$

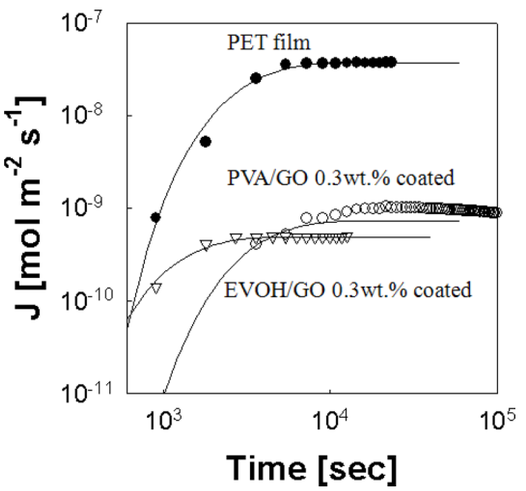

Fig. 4. Oxygen molar flux with respect to time of polyethylene terephthalate (PET), poly(vinyl alcohol) (PVA)/graphene oxide (GO) coated and ethylene vinyl alcohol (EVOH)/GO coated PET film.

where c* is the saturated oxygen concentration in the film, D is the oxygen diffusivity in the film, S is the oxygen solubility in the film, and P is the oxygen permeability [10].

The oxygen flux through the films is plotted with respect to time in Fig. 4. Model calculations by Eq. (1) fit the experimental data well. The oxygen diffusivity can be calculated from the slope of the straight line by Eq. (1). The oxygen solubility also can be calculated by Eq. (4). The oxygen molar flux of EVOH/GO (0.3 wt%) coated film is compared to the previous results for the PET and PVA/GO 0.3 wt% coated film by Kim et al. [10]. The oxygen molar flux of EVOH/GO (0.3 wt%) coated film is 123 times and 2 times lower than that of PET and PVA/GO (0.3 wt%) coated film [10]. We calculated the oxygen permeability of EVOH/GO and EVOH/RGO film without PET film by Eq. (5).

$$\frac{1}{P} = \frac{x_{GO}}{P_{GO}} + \frac{1-x_{GO}}{P_{PET}} \tag{5}$$

where x_{GO} is the ratio of the thickness of EVOH/GO to EVOH/GO/PET film. The oxygen permeability of EVOH/GO (0.3 wt%) film is 3.63×10^{-15} mol s^{-1} m^{-1} Pa^{-1}, which is 63% of that of the pure EVOH film. The oxygen permeability of EVOH/RGO (0.3 wt%) film is 4.48×10^{-15} mol s^{-1} m^{-1} Pa^{-1}, which is 78% of that of the pure EVOH film. The oxygen diffusivity of EVOH/GO (0.3 wt%) film is 1.4 times lower than that of the pure EVOH film.

The Nielsen approximation describes the increase in the tortuosity of the gas diffusion path by relating it to the volume fraction and aspect ratio of the crystal, as in the following equation [10,16]:

$$D = D_0\left(\frac{1-\phi_c}{1+\frac{\alpha}{2}\phi_c}\right) \tag{6}$$

where D_0 is the diffusivity of polymer, ϕ_c is the volume fraction of graphene, and α is the aspect ratio of graphene [10]. The aspect ratio is a function of the smallest dimension of the graphene

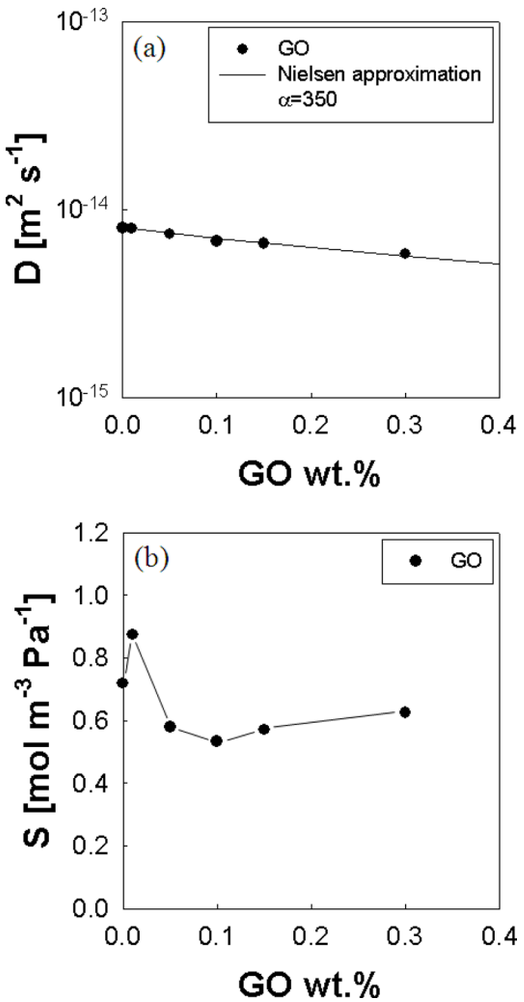

Fig. 5. Characteristics of oxygen permeation through ethylene vinyl alcohol/graphene oxide (GO) film. (a) Oxygen diffusivity. (b) Oxygen solubility.

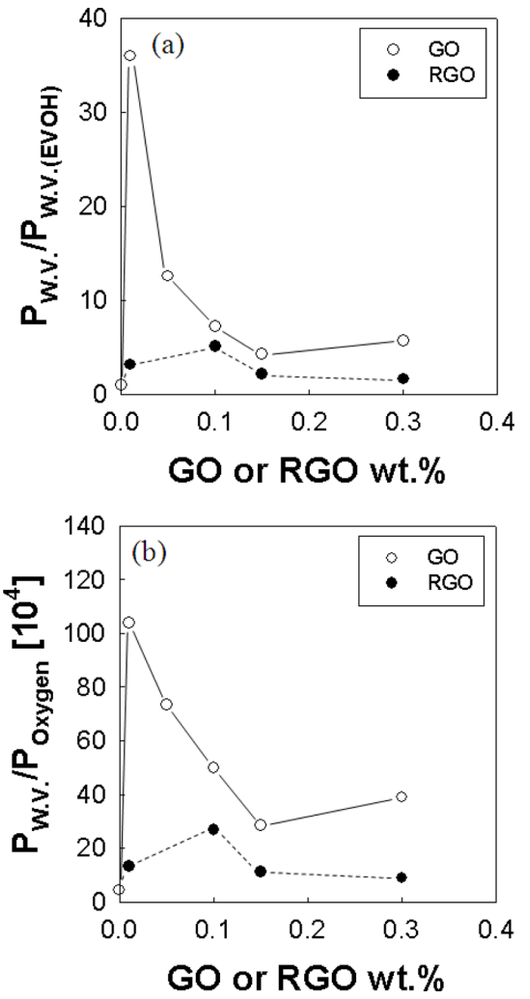

Fig. 6. Characteristics of water vapor permeation through ethylene vinyl alcohol (EVOH)/graphene oxide (GO) or EVOH/reduced GO (RGO) film. (a) Water vapor permeability of EVOH/GO or EVOH/RGO film normalized by permeability of EVOH film. (b) Ratio of water vapor permeability to oxygen permeability of EVOH/GO or EVOH/RGO film.

(α) and the intermediate dimension of the graphene (2R) [30]. The aspect ratio is defined as R/α [30]. The solid line in Fig. 5a shows that Eq. (6) describes the effect of impermeable crystal contents on the diffusivity with the aspect ratio of 350 for GO. The aspect ratio of GO can also be estimated from gas permeability of film. Lape and co-worker's model for membranes dispersed with impermeable anisotropic flakes in a random array gives [13,30]:

$$\frac{P}{P_0} = \frac{1-\phi}{\left(1+\frac{\alpha\phi}{3}\right)^2} \quad (7)$$

where P is the oxygen permeability of filled polymer, P_0 is the oxygen permeability of unfilled polymer, ϕ is the volume fraction of graphene, and α is the aspect ratio of graphene [13,30]. Model calculations fit the experimental data with the aspect ratio of 350 for GO, which is consistent to that obtained from oxygen diffusivity. In Fig. 5b, the oxygen solubility is initially decreased by adding a very small amount of GO into EVOH. This may be due to the modification of the structure of PVA crystalline by the addition of GO. The oxygen solubility is decreased by the further addition of GO into EVOH as seen in Fig. 5b.

In Fig. 6a, we plotted the relative value of water vapor permeability to EVOH. The water vapor permeability of RGO is lower than that of the GO. This may be due to the decrease of the interlayer spacing after reduction. Water molecules diffuse through the interlayer spacing [4], so the decrease of interlayer spacing may result in the reduced water vapor diffusivity. The decrease of water vapor permeability in the RGO/EVOH film compared to that of the GO/EVOH film may also be due to the decrease of oxygen to carbon ratio by the reduction. In Fig. 6b, EVOH/GO membranes exhibited 100 times improved (water vapor)/(oxygen) selectivity compared to EVOH pure membrane. These results point to the new possible applications of EVOH/GO films as an oxygen/water selective membrane.

DOI: http://dx.doi.org/10.5714/CL.2014.15.1.050

4. Conclusions

We prepared EVOH/GO membranes by solution casting method. XRD analysis showed GOs were fully exfoliated in the EVOH/GO membrane. The thermal properties of EVOH were modified by the hydrogen boding interaction between EVOH and GOs. The glass transition temperatures of EVOH/GO composites were increased by adding GOs into EVOH. Nominal melting temperatures of EVOH/GO composites were decreased by adding GOs into EVOH, indicating that GOs inhibit the crystallization of EVOH during non-isothermal crystallization. However, the equilibrium melting temperatures of EVOH were not changed by adding GOs into EVOH. The oxygen permeability of the EVOH/GO (0.3 wt%) film was reduced to 63% of that of pure EVOH film, with 84% light transmittance at 550 nm. The EVOH/GO membranes exhibited 100 times better (water vapor)/(oxygen) selectivity performance than pure EVOH membrane.

These results point to the new possible applications of EVOH/GO films as an oxygen/water selective membrane.

Acknowledgements

This work was supported by the research fund from Dong-A University.

References

[1] Mokwena KK, Tang J. Ethylene vinyl alcohol: a review of barrier properties for packaging shelf stable foods. Crit Rev Food Sci Nutr, **52**, 640 (2011). http://dx.doi.org/10.1080/10408398.2010.504903.

[2] López-Rubio A, Lagarón JM, Hernández-Muñoz P, Almenar E, Catalá R, Gavara R, Pascall MA. Effect of high pressure treatments on the properties of EVOH-based food packaging materials. Innov Food Sci Emerg Technol, **6**, 51 (2005). http://dx.doi.org/10.1016/j.ifset.2004.09.002.

[3] Mokwena KK, Tang J, Laborie MP. Water absorption and oxygen barrier characteristics of ethylene vinyl alcohol films. J Food Eng, **105**, 436 (2011). http://dx.doi.org/10.1016/j.jfoodeng.2011.02.040.

[4] Nair RR, Wu HA, Jayaram PN, Grigorieva IV, Geim AK. Unimpeded permeation of water through helium-leak–tight graphene-based membranes. Science, **335**, 442 (2012). http://dx.doi.org/10.1126/science.1211694.

[5] Bunch JS, Verbridge SS, Alden JS, van der Zande AM, Parpia JM, Craighead HG, McEuen PL. Impermeable atomic membranes from graphene sheets. Nano Lett, **8**, 2458 (2008). http://dx.doi.org/10.1021/nl801457b.

[6] Leenaerts O, Partoens B, Peeters FM. Graphene: a perfect nanoballoon. Appl Phys Lett, **93**, 193107 (2008). http://dx.doi.org/10.1063/1.3021413.

[7] Shin D, Bae SK, Yan C, Kang JM, Ryu JC, Ahn JH, Hong BH. Synthesis and applications of graphene electrodes. Carbon Lett, **13**, 1 (2012). http://dx.doi.org/10.5714/CL.2012.13.1.001.

[8] Hummers WS, Jr., Offeman RE. Preparation of graphitic oxide. J Am Chem Soc, **80**, 1339 (1958). http://dx.doi.org/10.1021/ja01539a017.

[9] Kovtyukhova NI, Ollivier PJ, Martin BR, Mallouk TE, Chizhik SA, Buzaneva EV, Gorchinskiy AD. Layer-by-layer assembly of ultrathin composite films from micron-sized graphite oxide sheets and polycations. Chem Mater, **11**, 771 (1999). http://dx.doi.org/10.1021/cm981085u.

[10] Kim HM, Lee JK, Lee HS. Transparent and high gas barrier films based on poly(vinyl alcohol)/graphene oxide composites. Thin Solid Films, **519**, 7766 (2011). http://dx.doi.org/10.1016/j.tsf.2011.06.016.

[11] Yang YH, Bolling L, Priolo MA, Grunlan JC. Super gas barrier and selectivity of graphene oxide-polymer multilayer thin films. Adv Mater, 25, 503 (2013). http://dx.doi.org/10.1002/adma.201202951.

[12] Kim H, Miura Y, Macosko CW. Graphene/polyurethane nanocomposites for improved gas barrier and electrical conductivity. Chem Mater, **22**, 3441 (2010). http://dx.doi.org/10.1021/cm100477v.

[13] Kim H, Macosko CW. Processing-property relationships of polycarbonate/graphene composites. Polymer, **50**, 3797 (2009). http://dx.doi.org/10.1016/j.polymer.2009.05.038.

[14] Shim SH, Kim KT, Lee JU, Jo WH. Facile method to functionalize graphene oxide and its application to poly(ethylene terephthalate)/graphene composite. ACS Appl Mater Interfaces, **4**, 4184 (2012). http://dx.doi.org/10.1021/am300906z.

[15] Welty JR, Wicks CE, Wilson RE. Fundamentals of Momentum, Heat, and Mass Transfer. 3rd ed., Wiley, New York, NY (1984).

[16] Polyakova A, Stepanov EV, Sekelik D, Schiraldi DA, Hiltner A, Baer E. Effect of crystallization on oxygen-barrier properties of copolyesters based on ethylene terephthalate. J Polym Sci B, **39**, 1911 (2001). http://dx.doi.org/10.1002/polb.1165.

[17] Wu Y, Peng X, Liu J, Kong Q, Shi B, Tong M. Study on the integrated membrane processes of dehumidification of compressed air and vapor permeation processes. J Membr Sci, **196**, 179 (2002). http://dx.doi.org/10.1016/S0376-7388(01)00564-6.

[18] Tabe-Mohammadi A. A review of the applications of membrane separation technology in natural gas treatment. Sep Sci Technol, **34**, 2095 (1999). http://dx.doi.org/10.1081/SS-100100758.

[19] Liu L, Chen Y, Kang Y, Deng M. An industrial scale dehydration process for natural gas involving membranes. Chem Eng Technol, **24**, 1045 (2001). http://dx.doi.org/10.1002/1521-4125(200110)24:10<1045::AID-CEAT1045>3.0.CO;2-T.

[20] Gebben B. A water vapor-permeable membrane from block copolymers of poly(butylene terephthalate) and polyethylene oxide. J Membr Sci, **113**, 323 (1996). http://dx.doi.org/10.1016/0376-7388(95)00133-6.

[21] George SC, Thomas S. Transport phenomena through polymeric systems. Prog Polym Sci, **26**, 985 (2001). http://dx.doi.org/10.1016/S0079-6700(00)00036-8.

[22] El-Dessouky HT, Ettouney HM, Bouhamra W. A novel air conditioning system: membrane air drying and evaporative cooling. Chem Eng Res Des, **78**, 999 (2000). http://dx.doi.org/10.1205/026387600528111.

[23] Scovazzo P, Burgos J, Hoehn A, Todd P. Hydrophilic membrane-based humidity control. J Membr Sci, **149**, 69 (1998). http://dx.doi.org/10.1016/S0376-7388(98)00176-8.

[24] Zhang Z, Mo Z, Zhang H, Wang X, Zhao X. Crystallization and melting behaviors of PPC-BS/PVA blends. Macromol Chem Phys, **204**, 1557 (2003). http://dx.doi.org/10.1002/macp.200350012.

[25] Nagara Y, Nakano T, Okamoto Y, Gotoh Y, Nagura M. Properties of highly syndiotactic poly(vinyl alcohol). Polymer, **42**, 9679 (2001). http://dx.doi.org/10.1016/S0032-3861(01)00493-1.

[26] Hoffman JD, Weeks JJ. Melting process and the equilibrium melting temperature of polychlorotrifluoroethylene. J Res Natl Inst Bur Stand A, **66**, 13 (1962).
[27] Lee HS. Size of a crystal nucleus in the isothermal crystallization of supercooled liquid. J Chem Phys, **139**, 104909 (2013). http://dx.doi.org/10.1063/1.4820560.
[28] Rogers WA, Buritz RS, Alpert D. Diffusion coefficient, solubility, and permeability for helium in glass. J Appl Phys, **25**, 868 (1954). http://dx.doi.org/10.1063/1.1721760.
[29] Ogasawara T, Ishida Y, Ishikawa T, Aoki T, Ogura T. Helium gas permeability of montmorillonite/epoxy nanocomposites. Composites A, **37**, 2236 (2006). http://dx.doi.org/10.1016/j.compositesa.2006.02.015.
[30] Lape NK, Nuxoll EE, Cussler EL. Polydisperse flakes in barrier films. J Membr Sci, **236**, 29 (2004). http://dx.doi.org/10.1016/j.memsci.2003.12.026.